J. Geophys. 42, 717–726, 1977

Journal of Geophysics

Micrometeoroid Data from the First Two Orbits of Helios 1

E. Grün[1]*, H. Fechtig[1], J. Kissel[1], and P. Gammelin[2]

[1] Max-Planck-Institut für Kernphysik, Saupfercheckweg, Postfach 1248, D-6900 Heidelberg, Federal Republic of Germany

[2] Electronic Projectierung, D-6948 Wald-Michelbach, Federal Republic of Germany

Abstract. For the first time interplanetary dust has been detected directly by the micrometeoroid experiment on board of Helios 1 as close as 0.3 AU from the Sun. The experiment contains two sensors with a total effective area of 120 cm^2. One sensor (south sensor) is facing the southern ecliptic hemisphere while the other sensor (ecliptic sensor) detects particles about the ecliptic plane. Particle impacts are reliably identified by the presence of three independent signals, measured upon impact, including time-of-flight spectra of the ions released.

A total of 58 distinct micrometeoroid impacts was detected during 352 days of experiments operation during the first two orbits. The rate of large impacts (impact charge greater than 10^{-13} Coulombs) increases steeply (a factor of approximately 20) between 1 AU and perihelion. Also the average impact speed is found to increase by a factor 2 to 3 in the same distance interval. Most impacts were detected by the ecliptic sensor when it was pointing in the direction of motion of Helios 1 (probe apex). In contrast to that the south sensor detected also many impacts when facing the probe antapex. About twice the number of small impacts were detected when the south sensor was facing the Sun compared with the antisolar direction. This result supports qualitatively the finding of the Pioneer 8 and 9 dust experiments that small particles are leaving the solar system on hyperbolic orbits.

Key words: Interplanetary dust – Micrometeoroids – Helios mission.

The Helios mission represents the first opportunity to measure micrometeoroids at closer than 0.75 AU heliocentric distance. This region of interplanetary space is of special interest since it was predicted that the spatial density of dust particles should increase close to the Sun due to the Poynting Robertson effect (Briggs, 1962) a force which causes the particles to spiral

* To whom offprint requests should be sent

towards the Sun and is one of the major loss mechanisms of particles in the zodiacal complex. Due to this higher spatial density the micrometeoroids collide more frequently with each other (Dohnanyi, 1976). Additionally comets, which are considered to be a major source for micrometeoroids, release most of their dust in the vicinity of the Sun (Whipple, 1955). All three effects can be more easily studied at 0.3 AU from the Sun than at the Earth's orbit.

1. Instrument Description

The micrometeoroid experiment on board Helios 1 measures the impact of individual dust particles. The experiment consists of 2 individual sensor units and a common electronic data processor. Figure 1 shows a schematic cross-section of the spaceprobe with the mounting positions of the two sensors. The spin axis of Helios is perpendicular to its orbital plane which is identical with the ecliptic plane. While the spacecraft spins around its axis with a period of 1 s the two sensors scan a full circle in azimuth. Two sensors are installed in order to allow a rough determination (two channels) of the ecliptic elevation of the paticle's orbits. The field of view of each sensor is a cone with approximately 60° half angle centered on the sensor axis. In elevation the field of view is limited by the spacecraft rim and by an external blind. One sensor (south sensor) is facing the southern ecliptic hemisphere and detects particles which have trajectory elevations from $-90°-10°$. The other sensor (ecliptic sensor) detects particles with elevations from $-45°-+55°$ with respect to the ecliptic plane.

The cross-section of the south sensor is shown in Figure 2. The sensor consists of the solar wind protection system, the impact ionisation detector and the time-of-flight spectrometer. Two small electronic boxes containing preamplifiers and high voltage power supplies are directly attached to the sensor. A detailed description has been given by Dietzel et al. (1973). Five quantities are generally measured if a micrometeoroid hits the venetian blind type target: (1) the total negative charge (electrons) (2) the total positive charge (ions) released upon the impact, (3) the rise-time of the negative charge pulse, (4) the rise time of the positive charge pulse and (5) the time-of-flight spectrum of the ions. The instrument is triggered when a signal exceeds the threshold of either the positive or negative charge channel. With the south sensor additionally the electrostatic charge (6) of the dust particles is measured by the charge induced on a grid in front of the target. The ecliptic-sensor is covered by a thin film (3,000 Å parylene coated with 750 Å aluminium) as protection against solar radiation. Here the time (7) is measured between the penetration of the film and the impact on the target.

Besides these parameters measured directly from the impact, additional information is gathered and transmitted to earth: (8) various coincidences between the measured signals, enabling one to discriminate between noise and "probable" impacts, (9) the time at which the event has occured, and (10) the pointing direction (azimuth) of the sensor. If a "probable" impact is indicated by the proper coincidences, the count on one out of four registers is increased by one, this register is selected according to the amplitude of the positive charge signal

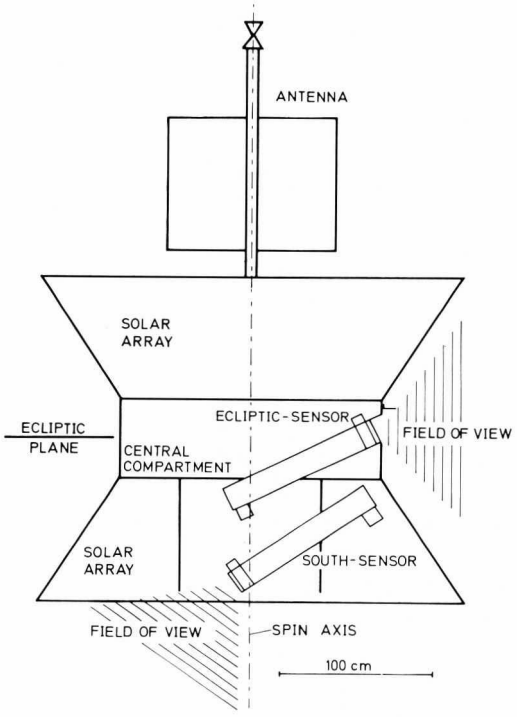

Fig. 1. Schematic view of the Helios spacecraft with mounting positions of the dual sensor micrometeoroid experiment

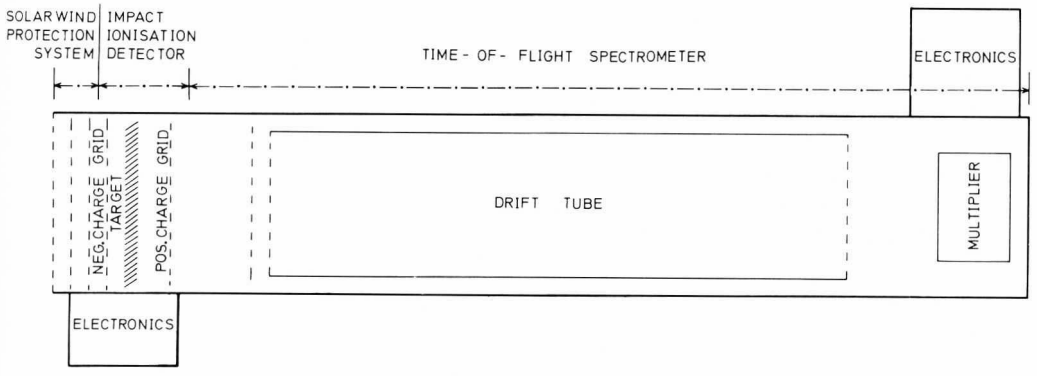

Fig. 2. The Helios micrometeoroid experiment, south sensor

(IA). By this method one obtains from the four counters the number of "probable" impacts within 4 positive charge intervals roughly corresponding to 4 different mass intervals of micrometeoroids. All the information on one event is contained in an experiment-data-frame of 256 bits which is transmitted to earth once every 20 s–20 min (depending on the Helios-Earth distance). The experiment worked satisfatorily, except for a total of 26 days during the first 3 months of the mission when the experiment was blocked in a non-measuring mode.

The experiment has a sensitivity threshold for micrometeoroids with masses of 3×10^{-13} g at an impact speed of 10 km/s. The measured parameters allow the determination of the particle mass, speed, electrostatic charge and composition of the plasma produced by the impact onto the sensor.

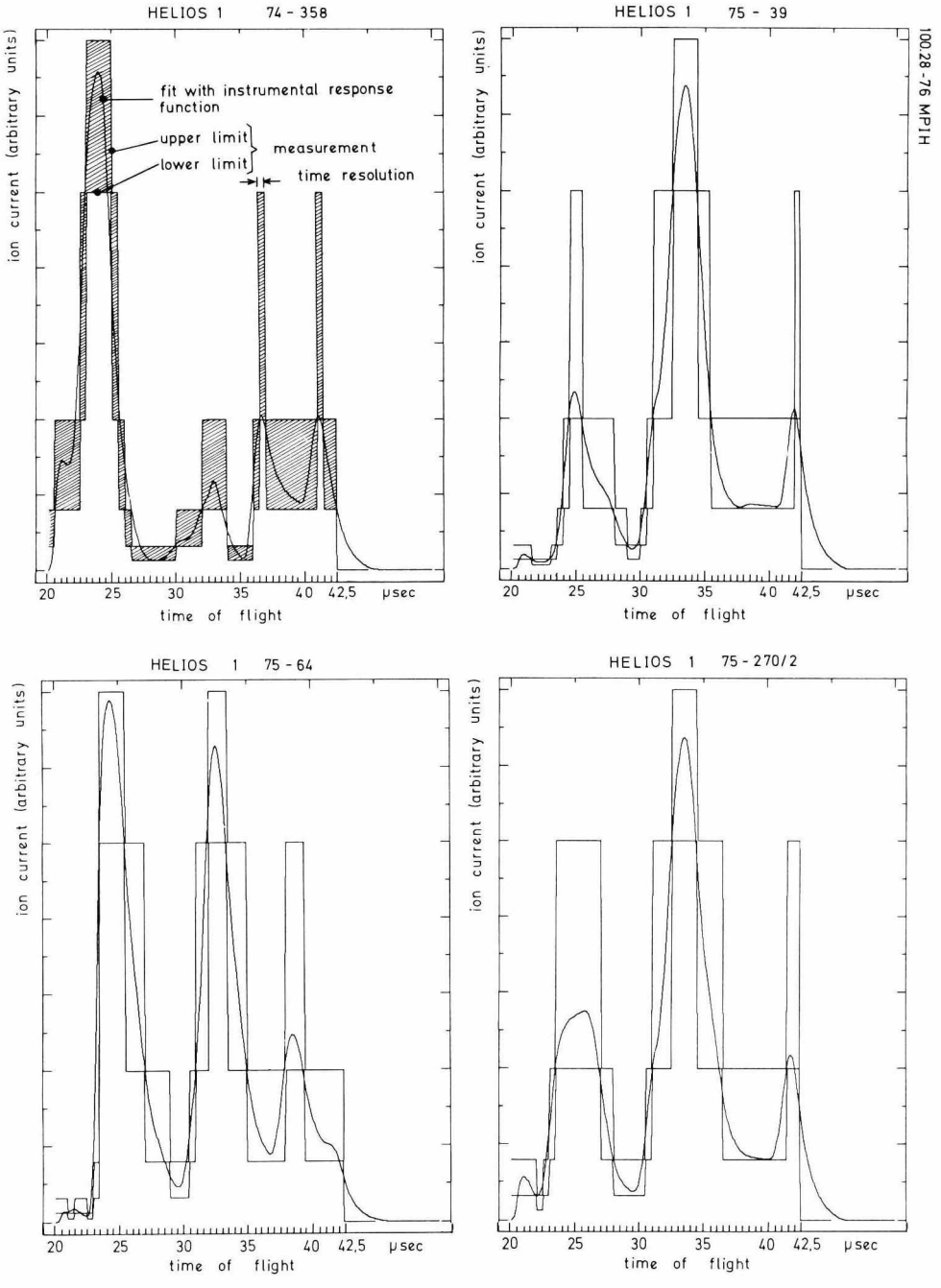

Fig. 3. Time-of-Flight spectra of ions released upon micrometeoroid impact onto the Helios sensors

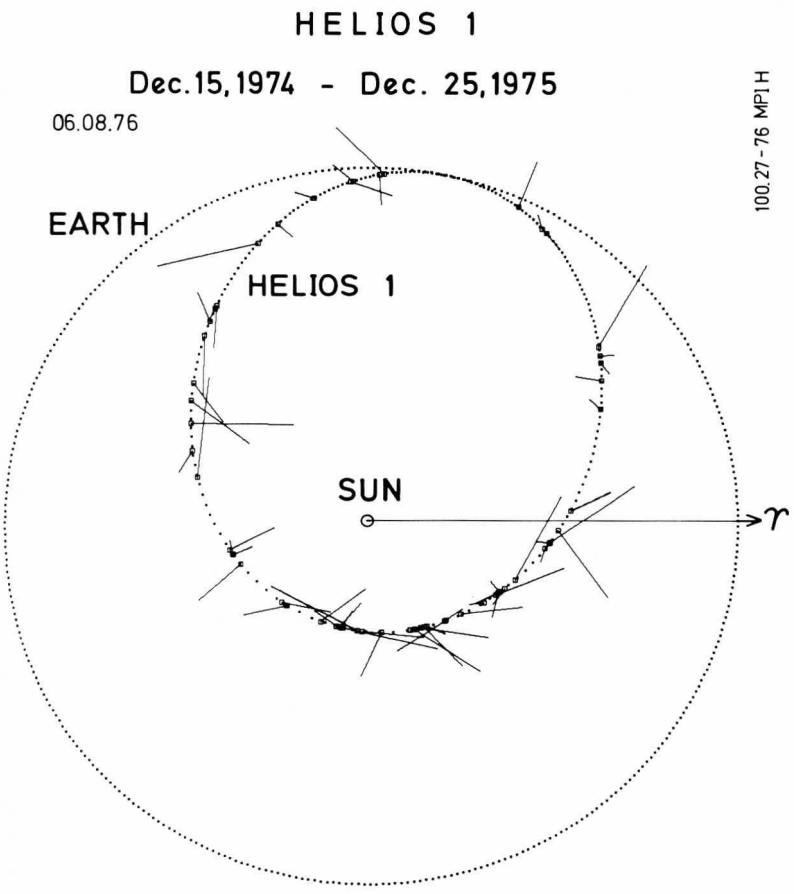

Fig. 4. Impacts detected during the first two orbits of Helios around the Sun (□). Bars attached to the small squares indicate the pointing direction of the experiment at the time of impact. The length of the bars represent the magnitude of the ion charge released upon impact

2. Impact Identification

The identification of an impact of a dust particle onto a sensor requires narrow time-coincidences between several signals measured from this event. These requirements were established and verified during the calibration of the instrument with artificially accelerated dust particles. The most affirmative coincidences are the occurrence of both the positive and negative charge signals within a 12 μs time interval and the subsequent measurement of a time-of-flight spectrum of the ions released upon impact. By the first criterion, the simultaneous occurrence of both the electron and ion signal, some 80 "probable" impact events were found in the data. Fifty-eight of these events had measurable time-of-flight spectra and were identified as "true" impacts. Figure 3 gives four examples of time-of-flight spectra as measured by Helios 1. The digitized output current of the multiplier is shown for the period from 22.5 μs–45 μs after the impact.

The upper and lower limit of the measurement refer to the uncertainties of the analog-to-digital conversion. A preliminary best fit of the data representing approximately the original time-of-flight spectrum is also shown. This fit takes into account the instrumental response function. At this stage of analysis the total ion charge contained in the spectrum is used only to identify true impact events. The evaluation of the spectra themselves is in progress. Laboratory studies of impact spectra were recently published by Dalman et al. (1977).

The fifty-eight impacts which were detected during the first two revolutions of Helios 1 around the Sun are shown in Figure 4. The dotted circle and ellipse give the orbits of the Earth and Helios 1, respectively. The distance between two adjacent dots represents the flight path during one day. Within this first year Helios 1 had completed two heliocentric orbits. The squares superimposed onto the Helios orbit mark the places where micrometeoroid impacts were observed and the direction of the bars attached to these squares represents the sensor pointing direction at the time of impact. Since the sensors have a field of view of approximately $\pm 60°$ around their axis, the true impact direction may deviate from the direction shown by as far as 60°. The length of the bars indicate the measured amount of positive charge (IA) produced upon impact. This charge is a measure of the combined effect of the particle mass and impact speed. The charge represented by the longest bars ($IA = 15$) is 10^4 times larger than the charge represented by the shortest bars ($IA = 0$).

The true number of micrometeoroid impacts onto the experiment within the first mission year is greater than the number of impacts detected in the data because of the incomplete data coverage and instrumental dead-time. The most complete set of data (better than 90% coverage) exists for larger impact events ($IA > 4$) because these events are reliably identified by the experiment itself and counted in special impact counters. All the events which have been recorded by these counters were found in the data and 30 of them were identified as true impact events. Small events ($IA \leqq 4$) which had triggered the appropriate counter were not completely found in the data received on ground. The data coverage for small impacts corresponds to approximately 70% of the available measurement time.

3. Results

One of the prime objectives of the Helios micrometeoroid experiment is the determination of the radial dependence of the impact rate. Figure 5 shows this result from the first two revolutions of Helios 1. The number of large impacts ($IA > 4$) per 0.1 AU interval normalized to the time spent in this distance interval is plotted versus the radial distance. The error bars represent the statistical $\pm\sigma$–error limit of the number of impacts and the 0.1 AU interval, respectively. The impact rate increases steeply with decreasing distance. Approximately 20 times more impacts were recorded at the 0.3 AU as compared with 1 AU. This increase can be fitted by a power law with an exponent of -2.5 ± 0.8. This impact rate on the experiment which has a total effective area of 120 cm^2 yields a micrometeoroid flux of 2.1×10^{-5} particles/m^2 s onto a sensor mounted

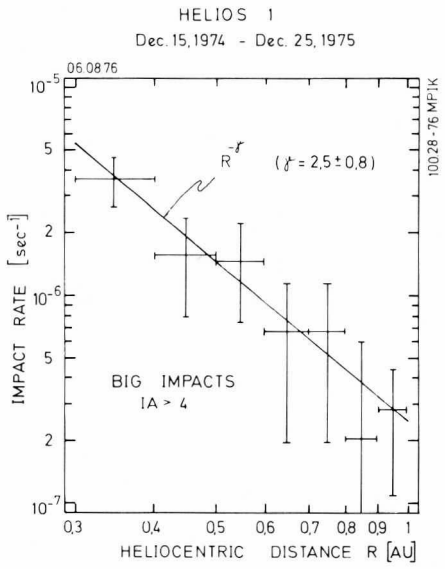

Fig. 5. Radial variation of the observed impact rate onto the Helios micrometeoroid experiment

on a spinning spacecraft at 1 AU distance from the Sun. This flux is within a factor of 2 of the flux as measured by the HEOS-2 satellite (Hoffmann et al., 1975) and comparable to the flux values derived from lunar crater statistics by Schneider et al., 1973). The latter fluxes correspond to micrometeoroids with masses greater than 10^{-12} g which is also the mass threshold for the impact charge IA = 4 at an impact speed of 10 km/s to 15 km/s.

The increase of the impact rate measured by this experiment can also be compared with the measurement of the zodiacal light from Helios 1. From these measurements Link et al. (1976), derived a spatial density of interplanetary dust at 0.3 AU which is 4–5 times the density obtained at 1 AU. The impact rate on a sensor is proportional to the spatial density multiplied with the average relative velocity between the sensor and the micrometeoroids. A preliminary analysis of the impact speed determined by the micrometeoroid experiment yields an increase of the average impact speed of a factor 2–3 between 1 AU and 0.3 AU.

This increase of the average impact speed at 0.3 AU causes a corresponding decrease in the minimum mass of particles detected by the sensor. The increase of the impact rate for a constant mass threshold will therefore be lower than the measured increase for constant charge threshold. Taking into account all these effects the measurements of interplanetary dust by the zodiacal light photometers and by the micrometeoroid experiment on board Helios 1 are compatible.

The pulse height distribution of the positive impact charge (IA) is shown in Figure 6. Impacts onto the ecliptic sensor are displayed separately from impacts on the south sensor. The linear pulse-height scale corresponds to a logarithmic impact charge scale covering a dynamic range of 10^4. Impacts with pulse-heights IA $\leqq 4$ are not complete and have to be corrected by a factor of approximately 1.5 in order to be comparable with big impacts (IA > 4). The number of big impacts

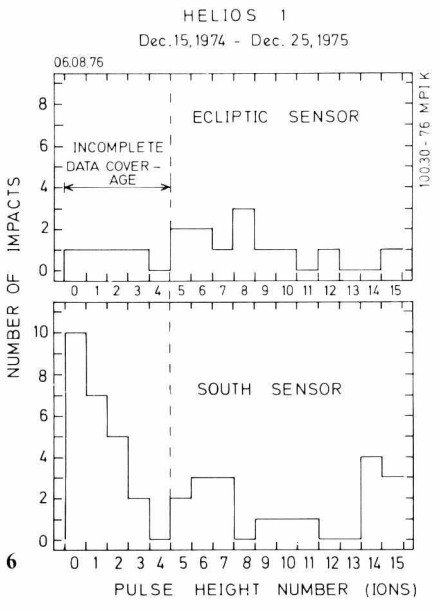

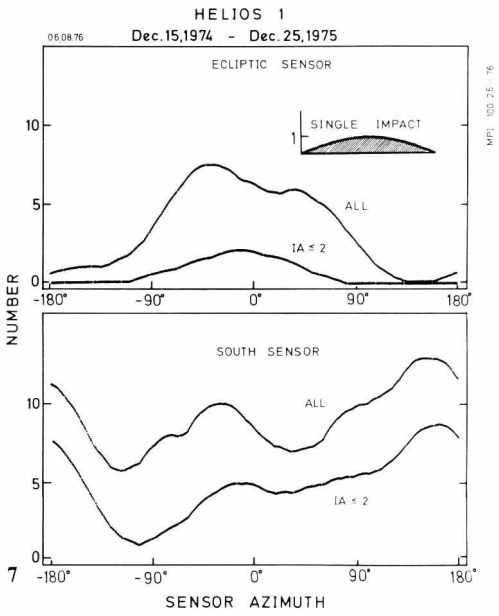

Fig. 6. Pulse hight distribution of the ion charge (IA) released upon impact

Fig. 7. Azimuthal distribution of impacts detected by Helios 1. A single impact is represented by an angular probability distribution centered on the sensor pointing direction at detection. The area of this function is shown in the upper right hand corner

on both sensors is similar within the statistical uncertainty indicating a wide distribution of dust orbit inclinations. Small impacts ($IA \leqq 4$) however, are counted 6 times more often by the south sensor than by the ecliptic sensor. This effect is attributed to the entrance film which covers the ecliptic sensor only and causes a cut-off in the detection limits of the smaller micrometeoroids. This film effect will be studied further in a laboratory program. As with the larger particles, the orbital inclination distribution of small micrometeoroids can not also be strongly concentrated to the ecliptic plane because impacts onto the south sensor require trajectory elevations greater than 10° with respect to the ecliptic plane.

Figure 7 shows the azimuthal distribution of dist impacts on both the ecliptic sensor and the south sensor. Each individual impact is represented by an area which corresponds to the angular sensitivity of the instrument as shown in the upper right hand corner of the graph. A sensor azimuth of 90° corresponds to a pointing of the sensor axis towards the Sun. 0° sensor azimuth points to the approximate apex direction of Helios. The impacts detected by the ecliptic sensor show a symmetric distribution peaking at the apex direction. In contrast to that a comparable number of impacts were detected by the south sensor from the antapex direction (180°).

The azimuthal distribution of small impacts $IA \leqq 2$ is asymmetric with respect to the apex direction. 15 impacts were detected while the sensor was pointing to

the solar hemisphere (0°–180°) compared with only 7 impacts from antisolar direction (−180°–0°). This finding supports the measurements from Pioneer 8 and 9 spaceprobes reported by Berg and Grün (1973) and McDonnell et al. (1975), who observed a concentration of large impacts from apex direction whereas small impacts were concentrated towards solar direction. Due to the high eccentric orbit of Helios a quantitative comparison requires a detailed analysis. The concept of this analysis is presented by Schmidt (1977).

Acknowledgements. The successful development, implementation and operations of this experiment would not have been possible without the collaboration of a great number of individuals from various departments of the Max-Planck-Institut für Kernphysik, from outside institutions and companies.

The authors are especially indebted to D. Linkert, W. Schneider, G. Dräger and Mrs. O. Kress for their personal engagement during that campaign. The support given to the instrument development, testing, calibration and project administration by D. Dörflinger, H. Geldner, S. Hägele, P. Kaiser, G. Matt, G. Ochmann, G. Schäfer, H. Schmidt, V. Träumer, H. Unser, H. Voth, H. Weber, W. Weiß and A. Zahlten is gratefully acknowledged. We thank for the support which we received by the project scientist Dr. H. Porsche.

The experiment was electronically developed, manufactured and tested by rfe Raumfahrtelektronik GmbH und Co. with a subcontract to Walter Fischer Gerätebau. The unremitting efforts and competent workmanship of F. Eckl, F. Eder, M. Steinich and their colleagues is gratefully appreciated.

The authors wish to thank J. Triolo from NASA Goddard Space Flight Center and Dr. M. Spivack from Union Carbide Corporation for their ingenious development and preparation of the crucial entrance film.

Careful attention and effective support to the experiment operations and data processing was given by J. Kehr and P. Piotrowsky and their teams of the German Space Operations Center (GSOC). The experiment was effectively coordinated with the Helios project by Drs. H. Dodeck, H.D. Dohmann, W. Kempe, K.O. Pfeiffer and P. Stampfl of the Gesellschaft für Weltraumforschung. Their contributions are gratefully acknowledged.

This work was supported by the Bundesminister für Forschung und Technologie with grant RS 10-7.

References

Berg, O.E., Grün, E.: Evidence of hyperbolic cosmic dust particles. Space Research XIII, M.J. Rycroft, S.K. Runcorn, eds., pp. 1047–1055. Berlin: Akademie-Verlag 1973

Briggs, R.E.: Steady-State space distribution of meteoric particles under the operation of the Poynting-Robertson effect. Astron. J., **67**, 710–723, 1962

Dalmann, B.K., Grün, E., Kissel, J., Dietzel, H.: The ion composition of the plasma produced by impact of fast particles. Planetary Space Sci., **25**, 135–147, 1977

Dietzel, H., Eichhorn, G., Fechtig, H., Grün, E., Hoffmann, H.-J., Kissel, J.: The HEOS A-2 and Helios micrometeoroid experiments. J. Phys. E: Sci. Instr. **6**, 209–217, 1973

Dohnanyi, J.S., Flux of hyperbolic micrometeoroids. In: Interplanetary dust and zodiacal light, H. Elsässer, H. Fechtig, eds. Lecture Notes Phys. **48**, pp. 170–180. Berlin-Heidelberg-New York: Springer 1976

Hoffmann, H.-J., Fechtig, H., Grün, E., Kissel, J.: First results of the micrometeoroid experiment S 215 on the HEOS-2 satellite. Planetary Space. Sci. **23**, 215–224, 1975

Link, H., Leinert, C., Pitz, E., Salm, N.: Preliminary results of the Helios A zodiacal light experiment. In: Interplanetary dust and zodiacal light, H. Elsässer, H. Fechtig, eds., Lecture Notes Phys. **48**, pp. 24–28. Berlin-Heidelberg-New York: Springer 1976

McDonnell, J.A.M., Berg, O., Richardson, F.F.: Spatial and time variations of the interplanetary microparticle flux analysed from deep space probes pioneers 8 and 9. Planetary Space. Sci. **23**, 205–214, 1975

Schneider, E., Storzer, D., Hartung, J.B., Fechtig, H., Gentner, W.: Microcraters on Apollo 15 and 16 samples and corresponding cosmic dust fluxes. Proc. Lunar Sci. Conf. 4th. **3**, 3277–3290, 1973

Schmidt, K.D.: Micrometeoroid orbits observable by the Helios experiment E 10. J. Geophys. 1977

Whipple, F.L.: A comet model, III. The zodiacal light. Astrophys. J. **121**, 750–770, 1955

Received January 31, 1977